Showcasing research on Magic Angle Coil Spinning (MACS) miniaturized detectors for nuclear magnetic resonance (NMR) from Dr. Vlad Badilita and Prof. Jan G. Korvink's team at the Institute of Microstructure Technology (IMT), Karlsruhe Institute of Technology (KIT), Germany.

Inductively coupled magic angle spinning microresonators benchmarked for high-resolution single embryo metabolomic profiling

The figure shows that many miniaturized MACS NMR detectors can be batch-fabricated by means of microstructuring in a robust and reproducible manner. Microfabrication techniques are being used to define high performance coils and capacitors, *i.e.*, the building blocks of a MACS detector. Miniaturized MACS NMR detectors are beneficial for the scientific community dealing with mass- and volume-limited, rare, or expensive samples. As an application example, this work has demonstrated, for the first time, ^{1}H NMR metabolic profiling of an intact single zebrafish embryo.

As featured in:

See Jan G. Korvink, Vlad Badilita *et al.*, *Analyst*, 2019, **144**, 7192.

ROYAL SOCIETY OF CHEMISTRY | Celebrating IYPT 2019

rsc.li/analyst

Registered charity number: 207890

Analyst

PAPER

View Article Online
View Journal | View Issue

Cite this: *Analyst*, 2019, **144**, 7192

Inductively coupled magic angle spinning microresonators benchmarked for high-resolution single embryo metabolomic profiling†

Shyam S. Adhikari,[a] Li Zhao,[b] Thomas Dickmeis,[c] Jan G. Korvink *[a] and Vlad Badilita *[a]

The magic angle coil spinning (MACS) technique has been introduced as a very promising extension for solid state NMR detection, demonstrating sensitivity enhancements by a factor of 14 from the very first time it has been reported. The main beneficiary of this technique is the scientific community dealing with mass- and volume-limited, rare, or expensive samples. However, more than a decade after the first report on MACS, there is a very limited number of groups who have continued to develop the technique, let alone it being widely adopted by practitioners. This might be due to several drawbacks associated with the MACS technology until now, including spectral linewidth, heating due to eddy currents, and imprecise manufacturing. Here, we report a device overcoming all these remaining issues, therefore achieving: (1) spectral resolution of approx 0.01 ppm and normalized limit of detection of approx. 13 nmol $s^{0.5}$ calculated using the anomeric proton of sucrose at 3 kHz MAS frequency; (2) limited temperature increase inside the MACS insert of only 5 °C at 5 kHz MAS frequency in an 11.74 T magnetic field, rendering MACS suitable to study live biological samples. The wafer-scale fabrication process yields MACS inserts with reproducible properties, readily available to be used on a large scale in bio-chemistry labs. To illustrate the potential of these devices for metabolomic studies, we further report on: (3) ultra-fine ^{1}H–^{1}H and ^{13}C–^{13}C *J*-couplings resolved within 10 min for a 340 mM uniformly ^{13}C-labeled glucose sample; and (4) single zebrafish embryo measurements through ^{1}H–^{1}H COSY within 4.5 h, opening the gate for the single embryo NMR studies.

Received 23rd August 2019,
Accepted 22nd October 2019

DOI: 10.1039/c9an01634a

rsc.li/analyst

Introduction

Since their invention in 2007,[1] magic angle coil spinning (MACS) micro-resonators have earned a special place among available NMR detectors for mass- and volume-limited samples. This is due to several advantages that are intrinsic to the very nature of these devices, which brought significant improvements in the way magic angle spinning (MAS) NMR measurements are being performed. MACS inserts are essentially tuned micro-resonators that are spun together with the sample. Resonance is achieved through the combination of a tiny inductor and a capacitor as two independent units,[1,2] or through a self-tuned coil design, the capacitance being distributed along the inductor.[3] The first advantage brought about by a MACS insert is the amplification of the magnetic flux in the sample region in comparison to the usual MAS NMR arrangement, achieved without any additional hardware modifications to the MAS probe. This leads to a sensitivity enhancement by a factor of 14 for a 4 mm MAS arrangement, as originally reported by Sakellariou *et al.*[1] Secondly, even if several different materials, *i.e.*, different magnetic susceptibilities, are packed in a relatively small volume, the corresponding line broadening is averaged out by the joint spinning of detector and sample.

Since their advent,[1] MACS inserts introduced several challenges that have been addressed, at least partially, over the past years. Fast spinning of the MACS detectors in a strong static magnetic field leads to the generation of eddy currents in the conductive materials of the insert, such as the capacitor terminals or the coil wire, which subsequently results in sample heating. This has consequences for sample viability (in the case of biological samples), and spectral quality, which deteriorates with a rise in temperature.

[a]*Institute of Microstructure Technology (IMT), Karlsruhe Institute of Technology (KIT), Hermann-von-Helmholtz-Platz 1, 76344 Eggenstein-Leopoldshafen, Germany. E-mail: jan.korvink@kit.edu, vlad.badilita@kit.edu*
[b]*Voxalytic GmbH, Rosengarten 3, 76228 Karlsruhe, Germany*
[c]*Institute of Toxicology and Genetics (ITG), Karlsruhe Institute of Technology (KIT), Hermann-von-Helmholtz-Platz 1, 76344 Eggenstein-Leopoldshafen, Germany*
†Electronic supplementary information (ESI) available. See DOI: 10.1039/C9AN01634A

Two reports[4,5] have investigated this aspect, deriving a numerical dependency of the dissipated heat on the spinning speed, as well as on the geometry of the solenoidal coil. These reports confirm the intuitive hypothesis that the dissipated power increases with both spinning speed and wire diameter. In fact, this limitation is apparent from several MACS papers where the reported spinning speeds are limited to 1500 Hz. Experiments performed for MAS rates of 250 to 5000 Hz show a clear worsening of the spectral resolution at these higher speeds using the splitting of the doublet of the anomeric proton of sucrose as a reference.[6] While several papers do report on MACS inserts built with 30 μm diameter wire,[6,7] hand-winding such delicate structures, and soldering or spot welding[8,9] their fine wire ends to a ceramic capacitor represents a bottleneck towards obtaining a large number of detectors in a robust manner and with reproducible performance.

Another issue in the design of MACS inserts is related to the mechanical balancing of the devices, a crucial property needed for fast spinning. Manual fabrication of the coil, and subsequent manual integration of a discrete capacitor, represents a built-in limitation due to lack of achievable precision. Microfabrication techniques showed great promise towards solving many of the original MACS issues: the use of an automatic coil winder facilitated robust integration of thin, 25 μm diameter wire, at the same time ensuring a precisely mechanically balanced device due to precise alignment by photolithographic patterning of the on-chip capacitor and sample holder.

However, in this case, solving one problem introduced another: the on-chip interdigitated capacitor implemented in the first generation of microfabricated MACS inserts[2] exhibited a low Q-factor of around 10 due to the high RF resistance of their long and thin metal parts. This compared unfavourably with the discrete capacitors used in the first MACS version, *i.e.*, ceramic capacitors with Q-factors as high as 10 000.[10] The low Q-factor of the microfabricated MACS inserts leads to decreased wireless signal transfer efficiency[11] of $\eta < 70\%$ between the microfabricated MACS insert and the MAS probehead coil. In a recent paper,[12] the efficiency has been increased to around $\eta = 88\%$ by re-designing the on-chip capacitor integrated with the wirebonded micro-coil.[13,14] Another type of microfabricated MACS insert design has been reported,[3] in which the capacitance is distributed between the windings of the coil. The maximum reported gain in sensitivity from these inserts was only about 3; the final assembly was done manually and therefore may also be prone to imbalances. In a recent paper,[12] we have confirmed that, for Q-factor values of the entire MACS micro-resonator chain higher than 20, the wireless coupling efficiency η between the micro-resonator and the MAS probehead coil exceeds 90%. Given the fact that typical values for the quality factor of the micro-coil are around 50,[13] this reduces the requirement on the microfabricated capacitor Q-factor to around 33, achieving a reasonable compromise in signal transfer efficiency between the microfabricated MACS insert and the MAS probehead coil.

In this paper, we aim to demonstrate that we have opened the previously mentioned bottleneck that has prevented MACS inserts from being widely adopted by practitioners. For an in-depth understanding of the performance of this MACS insert, of the differences with respect to previous or alternative MACS versions, as well as handling precautions, it is important that NMR spectroscopists from different application fields are aware of the design considerations and fabrication details.

A general characterization is presented in the **Benchmarking** section of the main text of the paper, covering basic aspects of an NMR detector: sensitivity gain with respect to MAS, spectral resolution, normalized limit of detection. The **Metabolomics** section reports for the first time HRMAS measurements on an intact single zebrafish embryo, being able to identify the main metabolites in less than 10 minutes scanning time. Harnessing strong RF irradiation from MACS microcoils has been demonstrated in the **Heteronuclear 2D NMR** section using ^{1}H decoupling for HMQC pulse sequences.

Experimental

Benchmarking

We present in this section the benchmarking of several key performance parameters: spectral resolution, overall sensitivity, and sensitivity gain obtained using the MACS inserts shown in Fig. 1. The ESI† contains additional electrical and thermal characterization of the microfabricated MACS inserts.

In order to evaluate the performance of the MACS insert, the NMR spectrum from a MACS device was directly compared to the NMR spectrum obtained with a dummy MACS insert,

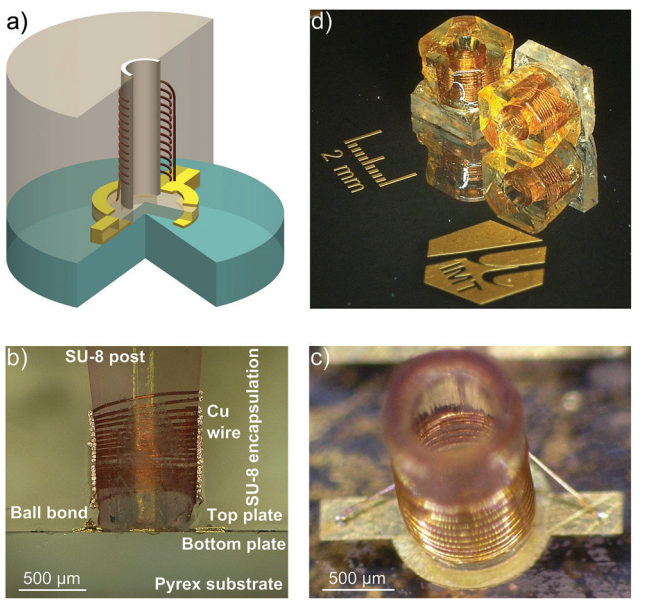

Fig. 1 (a) CAD rendering of the MACS insert showing the capacitor and the coil; (b) cut section of the MACS device; (c) a micro-coil wirebonded to the parallel plate capacitor; (d) final MACS detector separated from the substrate ready for experiment.

i.e., without MACS signal enhancement. A dummy MACS insert is an otherwise identical MACS device which does not contain a resonator coil. As a result, the sample volume is also 380 nl, but the RF excitation and signal reception are performed directly by the static MAS coil. All the NMR experiments were performed on a wide bore 11.7 T Bruker AVANCE III NMR spectrometer equipped with a 4 mm HRMAS probe.

RF amplification. The RF amplification and sensitivity enhancement achieved with the MACS insert have been determined using an adamantane sample (Sigma Aldrich). A nutation experiment, which is an array of NMR spectra at increasing pulse widths for a specified power level, serves to identify the π/2-pulse, RF field homogeneity, off-resonance effects and nonlinear pulse behaviour in a device. The ^{1}H nutation spectrum is shown in Fig. 2: a π/2-pulse at 24 W is achieved in 1.1 μs using the MACS insert (resonant at 463 MHz), *versus* 3.3 μs for a regular MAS experiment performed on the same amount of sample within a dummy MACS structure. The probe efficiency of these arrangements calculated from the measured nutation spectrum is around 1089 μT $W^{-0.5}$ and 363 μT $W^{-0.5}$, respectively. The ratio of the respective probe efficiencies leads to an RF field enhancement of approx. 3. By evaluating the ratio of amplitudes at 450°/90° from the nutation spectrum, an RF field homogeneity of 60% is obtained for the MACS inserts. The low B_1 field homogeneity of the insert suggest that the sample at the center of the container experiences a much stronger RF field than at the edges of the container. Additionally, this also means that a simpler pulse sequence (*e.g.* HMQC) would lead to better sensitivity than a complex sequence having multiple number of RF pulses (*e.g.* HSQC). This value can be improved by increasing the sidewall thickness of the sample containers, as well as limiting the sample region to the active region of the coil. However, increasing the sidewall thickness would lead to the reduction in the filling factor of MACS inserts. The B_1 field homogeneity from the commercial coil in the 4 mm MAS probehead is around 75%.

Sensitivity enhancement. For sensitivity enhancement measurements, experiments were conducted with a MACS (resonant at 466 MHz) and with a dummy insert at various spinning speeds, the signal being acquired from the same sample volume that fits inside the MACS insert, *i.e.*, 380 nl. The MACS and MAS NMR spectra from the adamantane sample at 3 kHz and 5 kHz are shown in Fig. 3. A factor of 6 gain in sensitivity can be achieved with the help of these resonant inserts. The signal-to-noise (SNR) ratio of an NMR experiment[15] for microscopic samples significantly depends on the geometry of the receiver coil (filling factor), as well on the excitation efficiency (B_1/i). Hence, due to the improved filling factor provided by the MACS inserts, a further improvement in the SNR is observed, in addition to the RF field gain.

It is important to note that the sensitivity enhancement reported here is not a limitation of the MACS insert,[16] but rather related to the limited range of the tuning and matching capacitors of the vendor-supplied MAS probe. MACS resonators in the range of 471 to 529 MHz could not be used for measurements due to the large magnitude splitting in the reflection curve induced by the coupling of MACS detectors with the coil in the MAS probe. Because of the limited capacitance range, the reflection curve could not be tuned and matched at 500 MHz. The limitation in the sensitivity gain to a factor of 6

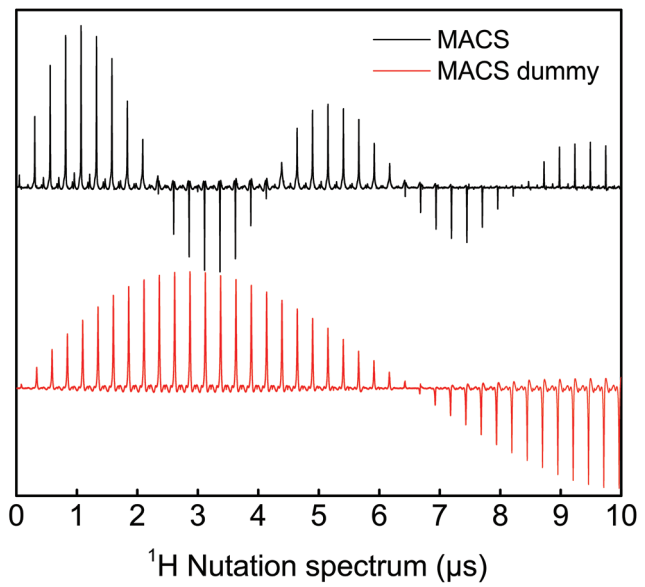

Fig. 2 Comparison of the nutation spectrum for MAS and MACS coils using a sample of adamantane at an excitation power of 24 W. The reduction in the π/2-pulse in the case of MACS gives an indication of the B_1 field enhancement inside the sample region. The ratio of amplitudes at 450°/90° from the nutation spectrum suggests an RF field homogeneity of 60% for the MACS inserts.

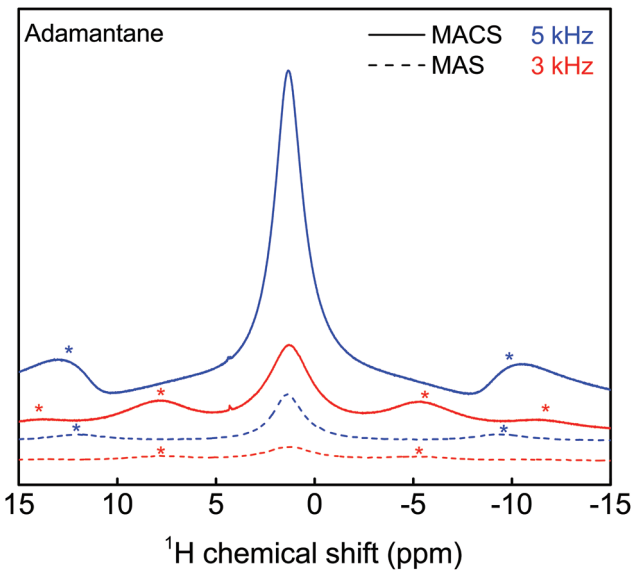

Fig. 3 Evaluation of the sensitivity enhancement achieved with a MACS insert using an adamantane sample at two spinning speeds (3 kHz and 5 kHz). The SNR improvement with the insert is estimated to be around 6 (see ESI section S4†). A π/2-pulse of 1.1 μs and 3.3 μs was used for the MACS and MAS experiments respectively at an excitation power was 24 W and 16 averages were taken.

in the present experimental setup is explained in more detail in section S4 of the ESI.†

Limit of detection and spectral resolution. Spectral resolution in miniaturised inductive NMR detectors is affected by the fact that multiple materials with various magnetic susceptibility values are typically packed in a limited volume, leading to a relatively large number of interfaces and the associated jumps in the B_0 field. At the same time, the spectral resolution requirements for, *e.g.*, ^{1}H NMR are rather tight: taking into account a proton chemical shift of about 10 ppm, in order to be able to employ NMR for metabolomic studies, where typically a large number of metabolites must be identified within a sample. A miniaturised detector would ideally deliver spectral linewidths better than 0.01 ppm. One MACS insert consists of the following materials: glass substrate, SU-8 epoxy as a constitutive material for the sample holder and coil support, metal for the on-chip capacitor and for the microcoil. A major improvement with respect to the previous version of microfabricated MACS resonators is represented by the encapsulation of the detector in SU-8 epoxy, *i.e.*, the same material as the sample holder. As a result, the air–epoxy interface is pushed further away from the sample, improving the homogeneity of the B_0 field in the sample region, thereby improving the overall spectral resolution.

Spectral resolution is also influenced by the sample temperature. In the case of MACS inserts, eddy currents arising within the electrically conductive components of the detector spinning rapidly within the B_0 field may lead to significant increase in the sample temperature and the subsequent degradation of spectral resolution.[6] Fig. S1 in the ESI† provides a comparative analysis using two different wire diameters for the wirebonded microcoil: 50 μm and 25 μm. While the gain in the quality factor due to the overall lower electrical resistance when using larger diameter wire is relatively moderate, the temperature penalty is significant. Measurements performed on the ethylene glycol spectrum show a 45 °C temperature difference between spinning at 7 kHz and 1 kHz when MACS microcoils are wound with 50 μm wire *versus* only 8 °C increase when MACS microcoils are wound with 25 μm wire (ref. section S4 ESI†). For the planar spiral microfabricated monolithic MACS inserts,[3] the estimated temperature rise at 7 kHz is about 5 °C. The improved thermal behaviour is due to reduced conductor thickness of 17 μm.

Fig. 4 shows a spectrum of a 500 mM sucrose sample in D_2O acquired from a MACS device, which has a resonance frequency of 470 MHz. The limit of detection and spectral resolution of the NMR experiment is evaluated from the doublet of the anomeric proton of sucrose. The SNR of this proton peak is calculated to be approx. 40. The acquisition time for the single scan experiment is taken to be 1 s. From these values, the normalized limit of detection[17] ($nLOD_\omega$) was evaluated to be approx. 13 nmol $s^{0.5}$ at 500 MHz. The concentration limit of detection ($cLOD_\omega$) as introduced by Finch *et al.*[18] in the framework of metabolite profiling is approx. 320 mM $s^{0.5}$. Although the value is quite high as compared to the one reported for stripline resonator,[18] this is mainly due to the small sample volume of the MACS device. A 30% splitting in the anomeric proton doublet peak was observed. The linewidth of the singlet proton peak was around 4 Hz. Moreover, comparing the SNR obtained from a similar volume of sucrose solution in a dummy MACS insert confirmed the factor of 6 sensitivity gain.

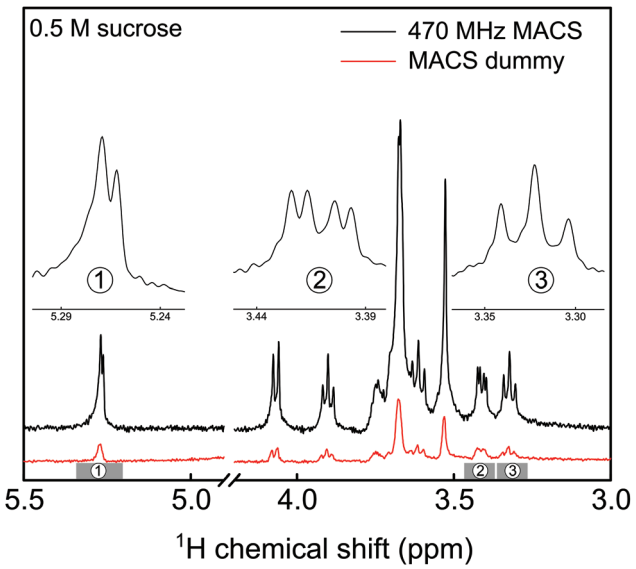

Fig. 4 Comparison of NMR spectrum of 500 mM sucrose obtained from a MACS and a dummy MACS insert acquired from a volume of 380 nl. A 30% splitting in the anomeric proton doublet peak was observed using a MACS insert and the singlet proton peak linewidth was around 4 Hz. A π/2-pulse of 1.1 μs and 3.3 μs was used for the MACS and MAS experiments respectively at an excitation power of 24 W and spinning speed of 3 kHz.

Metabolomics

One of the first attempts to perform metabolomic studies using MACS inserts was reported by Wong *et al.*[19] The authors evaluated the feasibility of handwound MACS detectors as a metabolomic tool by identifying metabolites from 500 μg of bovine muscle and human tissues, with a reported linewidth of 0.1 ppm. A second generation of handwound inserts[6] improved the spectral resolution down to 0.02 ppm for a 250 μg rabbit kidney tissue. The progress in the spectral quality was achieved by minimizing susceptibility and eddy current effects from the rotor insert and micro-coil, respectively. Further, these high resolution MACS (HR-MACS) inserts were used to perform metabolic profiling on intact organisms like yeast cells[20] and *Caenorhabditis elegans* worms.[7]

Microfabricated MACS inserts have emerged as a metabolic profiling tool, addressing the disadvantages mentioned above related to the fabrication and operation of handwound MACS inserts, and reporting linewidths of 1 ppm (ref. 2) and 0.1 ppm,[3] respectively. These findings on MACS inserts for metabolomics have been comprehensively summarized recently by Lucas-Torres and Wong.[21]

Although metabolomic studies have been performed on tissue samples, yeast cells and *C. elegans* worms, the potential

of MACS inserts on embryos which have a size similar to the detector geometry has not been explored. Embryonic stages of the zebrafish (*Danio rerio*) have become an increasingly used animal model[22] not only in developmental biology[23,24] and genetics,[25] but also for neuroscience,[26] human disease modeling,[27,28] drug development[29,30] and toxicology.[31] Several reporter tools have been explored[32] and among them HR-MAS experiments have been utilized for metabolic profiling, previously using 100 intact embryos inside the MAS rotor.[33,34] They were aged between 27 hpf (hours post fertilization) to 96 hpf and were spun at 5 kHz. The treatments were started at 3 hpf, but the measurements were done 24 hours later, hence at 27 hpf.

MACS inserts would bring significant enhancement in the detection of metabolites in these embryos. By allowing to assess inter-individual metabolite differences, MAS-NMR spectra of single zebrafish embryos would represent a significant advancement for metabolism studies in this model organism. Moreover, these miniaturized detectors would lead to a considerable decrease in the centrifugal forces experienced by the biological specimen during spinning. Hence, these inserts would constitute a powerful new tool for metabolic profiling of biological systems. 100 hpf stage zebrafish embryos (for ethics statement, refer section S1 ESI†), as shown in Fig. 5, are freely swimming in a 10 cm Petri dish (633180, Greiner Bio-One) containing E3 medium (refer section S1 ESI†), but do not yet require feeding, as they are relying on their yolk for nutrition.

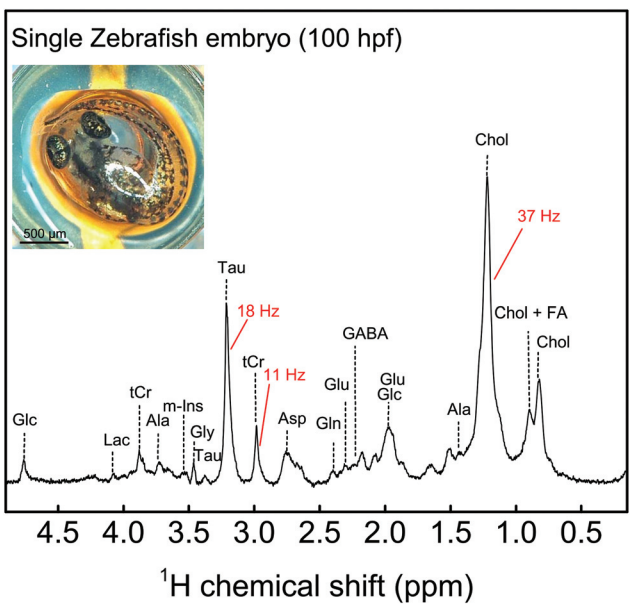

Fig. 5 ^{1}H MAS NMR spectrum of a single zebrafish embryo spun at 5 kHz after solvent suppression using a 20 μW pulse. The metabolic profile of the embryo shows a number of fatty acids, sugars *etc*. among other metabolites. The inset shows the photograph of an intact zebrafish embryo on top of the MACS orifice before loading. Ala, alanine; Asp, aspartate; Glc, glucose; Gln, glutamine; Glu, glutamate; Gly, glycine; Lac, lactate; Tau, taurine; m-Ins, (myo)-inositol, tCr, total creatine; GABA, gamma-aminobutyric acid; Chol, cholesterol; FA, fatty acid. A π/2-pulse of 1.1 μs at an excitation power of 24 W was used and 256 averages were taken with a repetition time of 1 s.

One of the embryos was first placed on top of a MACS device resonant at 467 MHz next to the orifice using a 20 μl Eppendorf pipette and tips (GELoader) as shown in Fig. 5 (for detailed information on embryo handling and sample filling, refer sections S1 and S3 ESI,† respectively). Subsequently, the embryo is successfully inserted into the sample volume of the 700 μm orifice MACS detector with the help of capillary force by absorbing the liquid inside. The rest of the sample volume is filled up with the E3 medium. Finally, the sample region is sealed at the top using a Biofilm tape (Applied Biosystems). ^{1}H NMR spectrum was initially obtained as shown in Fig. 5 under MAS conditions of 5 kHz. The solvent signal was suppressed using a pre-saturation pulse of 20 μW. The total experiment time was 6 min 30 s. Almost all the metabolites that have been reported from 100 embryos[33,34] have been identified in the ^{1}H NMR spectrum shown in Fig. 5. The assignment of metabolites was done by referencing the ^{1}H spectra of the compounds to previously reported data.[35,36] The metabolite peaks in the NMR spectrum have been referenced to trimethylsilyl propionate (TSP) solution. A two dimensional (2D) homonuclear correlation spectroscopy (COSY) experiment has been performed for improved clarity in the metabolite resonances in zebrafish embryos by helping to distinguish overlapping peaks. A calibration experiment was performed on uniformly ^{13}C-labeled glucose in D_2O to assess the performance of the MACS insert (refer section S7 ESI†). The COSY experiment was performed on an intact 105 hpf embryo. The spectrum as shown in Fig. 6 was acquired over a time period of 5 h 27 min

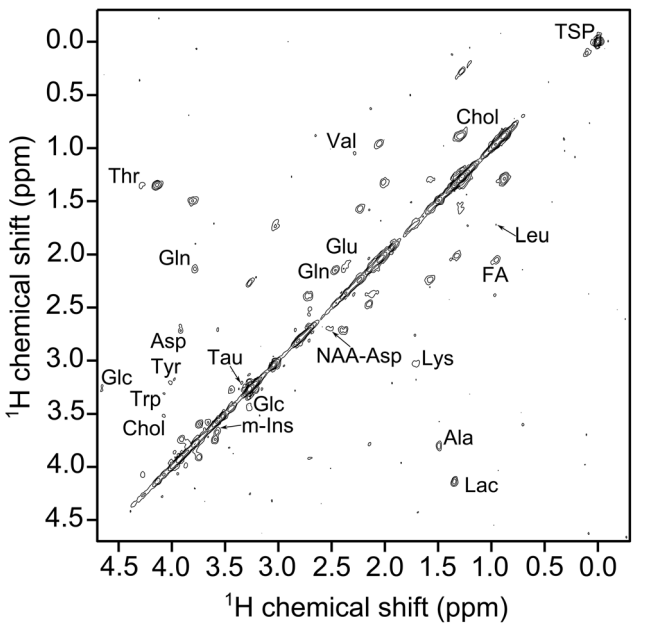

Fig. 6 ^{1}H–^{1}H COSY NMR spectrum of a single zebrafish embryo under MAS condition of 5 kHz after solvent suppression using a 20 μW pulse. Additional metabolites like tyrosine, leusine, L-tryptophan (Trp) *etc*. are detected. A π/2-pulse of 1.1 μs at an excitation power of 24 W was used. 512 t1 increments were collected with 32 averages and a relaxation delay of 1 s and 2048 data points were collected in the t2 domain over a spectral width of 5.5 kHz.

by collecting 2048 data points in the t2 domain over the spectral width of 5.5 kHz. 512 t1 increments were collected with 32 averages and a relaxation delay of 1 s. The acquisition time was 115 ms and suppression of the water resonance was done using a power of 20 μW. The COSY spectrum further reveals additional metabolites in the specimen compared to the 1D spectrum, and also the correlation between the metabolite peaks. All metabolite resonances are referenced with respect to the trimethylsilyl propionate (TSP) solution. The MACS signal enhancement revealed 80% of the metabolites as compared to previously published results, despite the acquisition of NMR signal from a single zebrafish embryo, in contrast to stronger metabolite signals from 100 embryos.[33,34]

Heteronuclear 2D NMR

A tuned MACS insert at 465 MHz was used for the 2D experiments. The ^{1}H nucleus was excited by the MACS coil at 24 W using a π/2-pulse length of 1.1 μs and the excitation of ^{13}C nuclei was done using the HRMAS probe coil at 50 W and ^{13}C π/2-pulse of 10 μs. The calibration experiments (refer section S8 ESI†) were performed on 2-^{13}C-labeled glycine sample (Sigma Aldrich). A cross polarization power of 24 W facilitates the polarization transfer from ^{1}H to ^{13}C spins in the glucose sample. A ^{1}H decoupling power of 10 W was used to decouple the ^{1}H spins from the ^{13}C spins, thereby allowing the removal of line broadening induced by heteronuclear dipolar and *J*-coupling. The spectral resolution of the ^{1}H NMR measurements is 7 Hz.

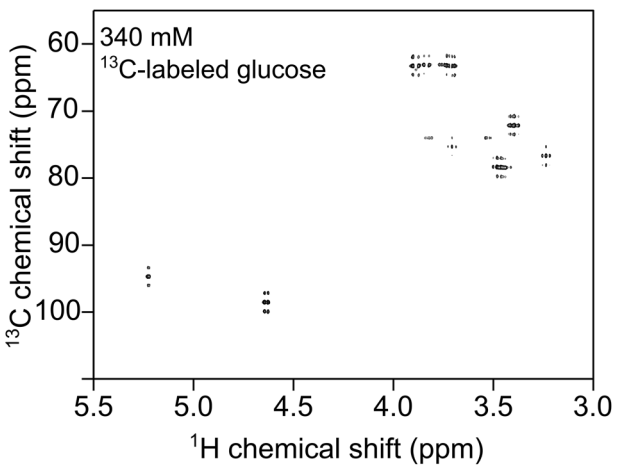

Fig. 7 2D HMQC NMR spectrum of 340 mM ^{13}C labeled glucose solution in D_2O showing ^{1}H–^{13}C correlations using a 380 nl ^{1}H MACS insert. The ^{1}H nucleus is excited by the MACS coil at 24 W using a π/2-pulse length of 1.1 μs and the excitation of ^{13}C nuclei is done using the HRMAS probe coil at 50 W and ^{13}C π/2-pulse of 10 μs. A ^{1}H decoupling power of 10 W is used to decouple the ^{1}H spins from the ^{13}C spins.

A 340 mM (0.13 μmol) uniformly ^{13}C-labeled glucose (Deutero GmbH) sample was used to perform a 2D HMQC experiment, which was acquired in 8 min 47 s and is shown in Fig. 7. The 2D HMQC experiment using a ^{1}H tuned MACS insert was introduced by Aguiar *et al.*[37] to apply the idea of inverse detection using MACS inserts to study low sensitive nuclei. The advantage of using ^{1}H tuned MACS inserts is that higher decoupling field strengths (250 kHz) can be applied at relatively lower power (25 W, refer section S6 ESI†). A fine *J*-splitting both in direct and indirect dimension is observed from Fig. 7. The excellent spectral resolution in a short measurement time allows extraction of more coupling information rather than peak assignments.

Conclusions

A microfabricated MACS insert has been presented here that is compatible with a 4 mm MAS system. The current device has been fully characterized with respect to its electrical properties, as well as to the temperature gradient/difference ($\nabla T/\delta T$) between the sample region and the periphery of the insert.

Table 1 provides a comprehensive overview of the single resonant MACS inserts reported so far: the initial MACS report[1] realized using a handwound coil and a discrete capacitor, an alternative MACS version from the same group based on a printed coil, the capacitor being realized through the distributed capacitance between the windings,[3] and the two types of wirebonded coils, one with on-chip interdigitated capacitors,[2] the other with the parallel plate on-chip capacitor.[12] A first inspection of this table shows that, except for the structure built using interdigitated capacitors, the other three devices show rather similar performance. The relatively lower performance in terms of spectral resolution exhibited by the printed coil MACS might be due to the properties of its constitutive materials, however it is worth noting that this device has the least eddy current heating. The spectral resolution delivered by the current device is comparable to the handwound MACS inserts. To see the present MACS device in a wider perspective, one might as well ask the question to which extent a MACS arrangement has a superior performance to an arrangement where both the rotor and the static coil are downscaled. In order to have a basis for comparison, the size of the coil must be considered as a common denominator. The only MAS technology comparable to the present MACS coil is the 0.7 mm

Table 1 Comparison of various MACS detectors for a 4 mm MAS system

	Capacitor	Coil	Wire thickness (μm)	δT at 5 kHz (°C)	Q_{MACS}	Resolution (ppm)	Sensitivity gain
MACS1 (ref. 1)	Discrete	Handwound	30	7	70	0.02	6.7–14
MACS2 (ref. 2)	Interdigitated	Wirebonded	25	—	—	1	—
MACS3 (ref. 3)	Parasitic	Printed	17	2.5	50	0.1	3.4
MACS4 (this work)	Parallel plate	Wirebonded	25	5	22	0.03	6

MAS system. MAS offers the advantage of faster sample spinning and eliminates the heating due to eddy currents from the spinning metallic parts (in the MACS case). However, downscaling the MAS experimental arrangement drastically decreases the filling factor of the probehead's detector coil (a filling factor of about 20% for 0.7 mm MAS technology) as opposed to significantly higher filling factors offered by the MACS technology (about 65% for the present MACS device).

The key contribution of this work, differentiating it from our previous advances, as well as from other approaches, is to demonstrate a MACS insert which is fabricated in a robust and reproducible manner by means of microstructuring, exploited in order to define high performance coils and capacitors, and therefore addressing the previous drawback of the first generation: its low quality factor *Q*. Microstructuring also offers the advantage that it eliminates any imprecision due to manual assembly, and ensures mechanically balanced devices, which is an important feature required for fast spinning speeds.

This paper marks the coming-of-age of MACS detectors, as their maturity enables a wide range of NMR applications involving fast sample spinning at high SNR, crucial to obtaining finely resolved spectra, thereby addressing multiple categories of practitioners. As an application example, this work has demonstrated, for the first time, ^{1}H NMR metabolic profiling of an intact single zebrafish embryo. The results revealed with HR-MACS are in good agreement with previous reports, proving the possibility of HR-MACS applications for low cell-count studies, as needed for example for human disease monitoring, drug development, or toxicity assessment.

For the future, a combination of slow spinning, joining MACS and the CMP (comprehensive multi-phase)-NMR[38] technique, could be applied to observe the metabolic activity of an intact single zebrafish embryo over a longer period of time through its multiple embryonic stages (*e.g.* from 10 hpf–100 hpf).

Conflicts of interest

Jan G. Korvink is a co-owner of Voxalytic GmbH, a startup company in Karlsruhe, Germany, that is commercialising a microfabricated MACS concept.

Acknowledgements

SSA, VB, and JGK acknowledge support from the European Research Council *via* the ERC Proof-of-Concept project LiVoX (680895). JGK acknowledges additional support from the ERC Senior Grant NMCEL (290586). VB acknowledges financial support from the DFG (Deutsche Forschungsgemeinschaft) Grant BA 4275/4-1. The authors would like to thank Dr Ali Moazenzadeh from Voxalytic GmbH for fruitful discussions and help with impedance measurements. This work was carried out with the support of Karlsruhe Nano Micro Facility (KNMF), a Helmholtz research infrastructure at Karlsruhe Institute of Technology (KIT).

References

1 D. Sakellariou, G. Le Goff and J.-F. Jacquinot, *Nature*, 2007, **447**, 694–697.
2 V. Badilita, B. Fassbender, K. Kratt, A. Wong, C. Bonhomme, D. Sakellariou, J. G. Korvink and U. Wallrabe, *PLoS One*, 2012, **7**, e42848.
3 J. A. Lehmann-Horn, J.-F. Jacquinot, J. C. Ginefri, C. Bonhomme and D. Sakellariou, *J. Magn. Reson.*, 2016, **271**, 46–51.
4 P. M. Aguiar, J.-F. Jacquinot and D. Sakellariou, *J. Magn. Reson.*, 2009, **200**, 6–14.
5 G. Aubert, J.-F. Jacquinot and D. Sakellariou, *J. Chem. Phys.*, 2012, **137**, 154201.
6 A. Wong, X. Li and D. Sakellariou, *Anal. Chem.*, 2013, **85**, 2021–2026.
7 A. Wong, X. Li, L. Molin, F. Solari, B. Elena-Herrmann and D. Sakellariou, *Anal. Chem.*, 2014, **86**, 6064–6070.
8 M. Inukai and K. Takeda, *J. Magn. Reson.*, 2010, **202**, 274–278.
9 K. Takeda, *Solid State Nucl. Magn. Reson.*, 2012, **47–48**, 1–9.
10 Exxelia group (Temex ceramics), Microwave components Product catalogue 157, 2015.
11 M. Utz and R. Monazami, *J. Magn. Reson.*, 2009, **198**, 132–136.
12 S. S. Adhikari, U. Wallrabe, V. Badilita and J. G. Korvink, *Concepts Magn. Reson., Part B*, 2018, **47**, e21362.
13 K. Kratt, V. Badilita, T. Burger, J. G. Korvink and U. Wallrabe, *J. Micromech. Microeng.*, 2010, **20**, 015021.
14 V. Badilita, K. Kratt, N. Baxan, M. Mohmmadzadeh, T. Burger, H. Weber, D. v. Elverfeldt, J. Hennig, J. G. Korvink and U. Wallrabe, *Lab Chip*, 2010, **10**, 1387–1390.
15 D. Hoult and R. Richards, *J. Magn. Reson.*, 1976, **24**, 71–85.
16 J.-F. Jacquinot and D. Sakellariou, *Concepts Magn. Reson., Part A*, 2011, **38**, 33–51.
17 V. Badilita, R. C. Meier, N. Spengler, U. Wallrabe, M. Utz and J. G. Korvink, *Soft Matter*, 2012, **8**, 10583–10597.
18 G. Finch, A. Yilmaz and M. Utz, *J. Magn. Reson.*, 2016, **262**, 73–80.
19 A. Wong, B. Jimenez, X. Li, E. Holmes, J. K. Nicholson, J. C. Lindon and D. Sakellariou, *Anal. Chem.*, 2012, **84**, 3843–3848.
20 A. Wong, C. Boutin and P. M. Aguiar, *Front. Chem.*, 2014, **2**, 38.
21 C. Lucas-Torres and A. Wong, *Metabolites*, 2019, **9**, 29.
22 G. J. Lieschke and P. D. Currie, *Nat. Rev. Genet.*, 2007, **8**, 353.
23 V. E. Prince, R. M. Anderson and G. Dalgin, *Current topics in developmental biology*, Elsevier, 2017, vol. 124, pp. 235–276.
24 G. Wang, S. K. Rajpurohit, F. Delaspre, S. L. Walker, D. T. White, A. Ceasrine, R. Kuruvilla, R.-j. Li, J. S. Shim, J. O. Liu, *et al.*, *eLife*, 2015, **4**, e08261.
25 S. H. Lam, Y. L. Wu, V. B. Vega, L. D. Miller, J. Spitsbergen, Y. Tong, H. Zhan, K. R. Govindarajan, S. Lee, S. Mathavan, *et al.*, *Nat. Biotechnol.*, 2006, **24**, 73.

26 M. Qi, M. C. Philip, N. Yang and J. V. Sweedler, *ACS Chem. Neurosci.*, 2017, **9**, 40–50.
27 P. Gut, S. Reischauer, D. Y. Stainier and R. Arnaout, *Physiol. Rev.*, 2017, **97**, 889–938.
28 P.-Y. Lam and R. T. Peterson, *Curr. Opin. Chem. Biol.*, 2019, **50**, 37–44.
29 A. Ordas, R.-J. Raterink, F. Cunningham, H. J. Jansen, M. I. Wiweger, S. Jong-Raadsen, S. Bos, R. H. Bates, D. Barros, A. H. Meijer, *et al.*, *Antimicrob. Agents Chemother.*, 2015, **59**, 753–762.
30 C. A. MacRae and R. T. Peterson, *Nat. Rev. Drug Discovery*, 2015, **14**, 721.
31 K. A. Horzmann and J. L. Freeman, *Toxicol. Sci.*, 2018, **163**, 5–12.
32 T. Dickmeis, Y. Feng, M. C. Mione, N. Ninov, M. Santoro, H. P. Spaink and P. Gut, *Front. Cell Dev. Biol.*, 2019, **7**, 15.
33 J. P. Berry, U. Roy, A. Jaja-Chimedza, K. Sanchez, J. Matysik and A. Alia, *Zebrafish*, 2016, **13**, 456–465.
34 U. Roy, L. Conklin, J. Schiller, J. Matysik, J. P. Berry and A. Alia, *Sci. Rep.*, 2017, **7**, 17305.
35 J. L. Markley, M. E. Anderson, Q. Cui, H. R. Eghbalnia, I. A. Lewis, A. D. Hegeman, J. Li, C. F. Schulte, M. R. Sussman and W. M. Westler, *et al.*, *Biocomputing 2007*, World Scientific, 2007, pp. 157–168.
36 M. T. Akhtar, M. Y. Mushtaq, R. Verpoorte, M. K. Richardson and Y. H. Choi, *Omics*, 2016, **20**, 42–52.
37 P. M. Aguiar, J.-F. Jacquinot and D. Sakellariou, *Chem. Commun.*, 2011, **47**, 2119–2121.
38 Y. L. Mobarhan, B. Fortier-McGill, R. Soong, W. E. Maas, M. Fey, M. Monette, H. J. Stronks, S. Schmidt, H. Heumann, W. Norwood and A. J. Simpson, *Chem. Sci.*, 2016, **7**, 4856–4866.